Low latitude Holocene hydroclimate derived from lake sediment flux and geochemistry

Adrian G Parker*[1], Gareth W Preston[1] Ash Parton[1], Helen Walkington[1], Phillip E. Jardine[2], Melanie J. Leng[3,4], Martin J. Hodson[5]

[1]*Human Origins and Palaeoenvironments Research Group, Department of Social Sciences, Oxford Brookes University, Headington, Oxford, OX3 0BP, UK.*

[2]*Palaeoenvironmental Change Research Group, Department of Environment, Earth & Ecosystems, The Open University, Walton Hall, Milton Keynes MK7 6AA, UK*

[3]*NERC Isotope Geosciences Facilities, British Geological Survey, Keyworth, Nottingham, NG12 5GG, UK*

[4]*Centre for Environmental Geochemistry, University of Nottingham, Nottingham, NG7 2RD, UK*

[5]*School of Health and Life Sciences, Oxford Brookes University, Headington, Oxford, OX3 0BP, UK*

* *Corresponding author*

Human Origins and Palaeoenvironments Research Group, Department of Social Sciences,, Oxford Brookes University, Headington, Oxford, OX3 0BP, United Kingdom. Tel.: +44 1865 483753; Fax: +44 1865 483937 Email address: agparker@brookes.ac.uk

ABSTRACT

This study investigates hydrological responses to climatic shifts using sediment flux data derived from two dated palaeolake records in southeast (SE) Arabia. Flux values are generally low during the early Holocene humid period (EHHP) (~9.0 to 6.4 k cal a BP) although several short-lived pulses of increased detrital input are recorded, the most prominent of which is dated between ~8.3 and 7.9 k cal a BP. The EHHP is separated from the mid-Holocene humid period (MHHP) (~5.0 to 4.3 k cal a BP) by a phase of increased sediment flux and aridity, which began between ~6.4 and 5.9 k cal a BP and peaked between ~5.2 and 5.0 k cal a BP. The termination of the MHHP is marked by a phase of high detrital sediment flux between ~4.3 and 3.9 k cal a BP. Whilst long-term shifts in climate are most likely linked to changes in the summer position of the Intertropical Convergence Zone (ITCZ) and associated Indian and African monsoon systems, it is noted that the abrupt, short-term phases of aridity observed in both records are coeval with intervals of rapid climate change globally, which triggered non-linear, widespread landscape reconfigurations throughout SE Arabia.

KEYWORDS

Arabia, sediment flux, Holocene, geochemistry, palaeolake

INTRODUCTION

It has long been recognised that the world's low latitude regions were characterised by significant hydrological changes during the Late Glacial and Holocene in response to the shifting position of the Intertropical Convergence Zone (ITCZ) and associated monsoon rains (Sirocko *et al.*, 1993; deMenocal *et al.*, 2000; Fleitmann *et al.*, 2007; Tierney and deMenocal, 2013;

Shanahan *et al*., 2015). Indeed, pioneering research by Alayne Street-Perrott documented widespread shifts in water balance from closed basin lakes in Africa, demonstrating major variations in rainfall and streamflow (Street and Grove, 1976, 1979). Her early work showed that the markedly arid conditions that characterised intertropical Africa during the Last Glacial Maximum (LGM) were followed by an early Holocene humid phase in which annual precipitation between 24°N and 8°S increased significantly. Further work suggested that these changes were driven by minimum precession and maximum insolation in the Northern Hemisphere (NH) (Kutzbach and Street-Perrott, 1985). The development of the Oxford Lake Level Data Bank (Street-Perrott *et al*., 1989) led to the compilation of records of lake status, a measure of relative water depth (low, intermediate, high), for lake basins that would have been closed for part, or all, of their late Quaternary history. This work suggested that high NH summer insolation in the early to mid-Holocene enhanced the thermal contrast between land and sea, with the resultant strengthening of the summer monsoon systems leading to high lake levels and the re-adjustment of vegetation across both hemispheres (Street-Perrott and Harrison, 1984, 1985; Kutzbach and Street-Perrott, 1985). Furthermore, palaeoclimate records from central and northern Africa suggested that orbital forcing alone was insufficient to produce conditions wetter than today (Yu and Harrison, 1996) and that positive feedback drivers also contributed to enhanced rainfall. Street-Perrott and Perrott (1990, 1993) demonstrated that closed lakes in the tropics and subtropics amplify climatic signals and are thus excellent indicators of variations in water budget. They suggested that short-term variations, which tend to reflect regional hydrological perturbations that are superimposed on more long-term, orbital variability, were coincident with injections of fresh water into the North Atlantic.

The climate of the Arabian Peninsula is complex and results from the interaction of major atmospheric systems, namely the ITCZ and associated monsoon circulation, as well as mid-latitude Westerlies (MLW). Consequently the region is a key area for understanding climate change in low-latitude regions during the Late Glacial and Holocene. However, in comparison to other low latitude deserts, such as the Sahel-Sahara, few independent, age-constrained, high-resolution records are available from Arabia, and those there are have revealed significant regional heterogeneity (sensu Thomas *et al*., 2012) during the Holocene (Berger *et al*., 2012). Speleothem records from Oman provide a detailed insight into Holocene hydrological changes caused by long-term shifts in the position of the summer ITCZ (Neff *et al*., 2001; Fleitmann *et al*., 2007). However, coming from mountain locations relatively close to the ocean and marginal to the peninsula as a whole, these records cannot readily be translated into evidence of wetter landscape conditions in the interior. Also emerging is a well-dated record of multiple periods of dune activity during the Holocene, derived from accumulation luminescence chronologies from sediment cores in Oman (Preusser *et al*., 2002), Liwa (Stokes and Bray 2005), and major dune-sediment exposures throughout northern areas of the United Arab Emirates (UAE) (Atkinson *et al*. 2011, 2012). Gaps in dune accumulation cannot be interpreted, without other evidence, to represent wetter phases *per se* (Thomas and Burrough 2012, Leighton *et al.* 2014), and may be controlled by sediment supply rather than climate (Preusser 2009). Thus while a better framework of Arabian Holocene environments is emerging, the record, for the purposes of addressing critical questions relating to landscape response, is either spatially limited (and therefore at risk of over-extrapolation) or difficult to reconcile as a clear proxy of hydrological change.

This paper presents new data from two key sites of Holocene climate variability in southeast (SE) Arabia; Awafi palaeolake and Wahalah palaeolake (Fig. 1). Previous work has determined that lacustrine conditions developed at both sites during the early to mid-Holocene, during which a series of pronounced changes in lake hydrology, vegetation dynamics and landscape stability are recorded (Parker *et al*., 2004, 2006; Preston *et al*., 2015). The site chronologies presented in these studies were based on a relatively simple age-depth model (linear interpolation), the drawbacks of which have been well documented (Telford *et al*., 2004; Blaauw, 2010). Street-Perrott *et al*. (2007) highlighted the importance of applying mass accumulation rates (MAR) and understanding changes in organic, siliclastic and biogenic mineral component flux rates to sediment sequences as they overcome distortions resulting from variable sedimentation rates and dilution effects (e.g. Barker *et al*., 2001; Ficken *et al.,* 2002; Cockerton *et al*., 2014). In this paper, we present a strengthened chronological framework for both sites based on a Bayesian age-depth model, which in turn allows the calculation of MAR and sediment flux data against which the existing palaeoclimate evidence from the region can be compared.

Environmental setting: climate and geomorphology

The study area is located in the northern United Arab Emirates (UAE), on the eastern margin of the Arabian Peninsula (Fig. 1). The region presently experiences an arid to hyper-arid desert climate, characterised by cool winters and hot summers. While highly variable, mean annual precipitation (~120 mm/year) is somewhat higher compared to coastal areas further to the south (e.g. ~80 mm/year in Dubai) (Parker *et al*., 2006), highlighting the significant orographic effect of the al-Hajar Mountains on precipitation gradients. Precipitation is highest during the winter months and is associated with MLW that originate in the Mediterranean and lead to increased

cyclogenesis throughout the eastern Mediterranean, the Red Sea and northern Arabia (Fisher and Membery, 1998). The wind regime is dominated by the low-level *Shamal* winds, which peak during the summer months as they blow from the northwest to southeast down the Arabian Gulf before turning clockwise across the Rub' al-Khali (Glennie and Singhvi, 2002). The study region is located to the north of the notional summer position of the ITCZ (Fig. 1), with monsoon-sourced rainfall presently limited to southern margins of the Peninsula (e.g. Yemen Highlands).

The geomorphology of the northern UAE is highly varied and comprises a mixture of desert, mountain, piedmont, and coastal environments (Parker and Goudie, 2008; Preston *et al*., 2012). The region is largely covered by Quaternary dune features belonging to the Rub' al-Khali sand sea (560,000 km^2), which extend into the area between the Arabian Gulf coastline (west) and the al-Hajar Mountains (east) (Fig. 2). Provenance studies of the dune sands in the UAE have shown that both are major sources of carbonate in the region, with the latter also contributing ultramafic igneous material. Iron-rich quartz grains, derived from the Arabian continental interior, are a third major component of the region's dune sands (El-Sayed, 1999; White *et al*., 2001; Farrant *et al*., 2012). A vast bajada of alluvial fans has developed where upland drainage systems emanate from the mountain front (Fig. 2).

Awafi palaeolake (25° 42' 57" N, 57° 55' 57" E; 6 m above sea level), initially revealed in the 1990s as a consequence of industrial quarrying, is a flat inter-dune depression (~2 km^2). The basin is bounded by northeast to southwest trending mega-linear ridges. There are no obvious surface inlets or outlets and so the basin is considered to have been hydrologically closed, with its main catchment area (ca. <5 km^2) composed of the surrounding permeable dunes sands. The

current depth to groundwater in the region is estimated to be ≤15 m (Alsharhan *et al*., 2001; p. 206). Sediment samples for this study were collected from an exposed sequence of over 2 m of stratified marls, silts and sands (Fig. 3), immediately adjacent (<1 m) to the original section analysed by Parker *et al*. (2004, 2006).

Wahalah palaeolake (25° 38' 48" N, 55° 47' 26" E; 10 m above sea level), located approximately 18 km to the southwest of Awafi, is also a dry, inter-dune depression (~2.4 km^2). The basin is considered to have been hydrologically closed with an overall catchment area of <5 km^2, and is bounded by mega-linear ridges. Similar to Awafi, there is no surface water at the site, with the groundwater table estimated to be well below the present day surface (≤15 m) (Alsharhan *et al*., 2001; p. 206). Sediment samples for this study were collected from a 2 x 2 m trench dug into the centre of the basin using a mechanical digger (Fig. 4).

Methods

Prior to sampling, the sediment sections at both sites were cleaned and logged using standard sedimentological techniques. Contiguous 1 cm samples were then extracted for further laboratory analysis to depths of 2.55 m and 2.14 m at Awafi and Wahalah respectively.

Mass specific, low frequency magnetic susceptibility (MS) measurements were made using a Bartington MS2 meter with an MS2B sensor at 0.1 SI unit sensitivity (Dearing, 1999). Dry bulk density (DBD) (g cm^{-3}) was measured as the dry weight of sediment per unit volume using the method outlined in Parker (1995, pp. 67–68). Organic matter (OM) was calculated by loss-on-ignition (LOI) (Heiri *et al*., 2001) and is reported as mass in mg $cm^{-2}a^{-1}$. Magnetic susceptibility,

DBD and OM measurements were made on each sample. For particle size analysis, samples were taken at 5 cm intervals and treated with 30% hydrogen peroxide to remove organic matter before being soaked overnight in a solution of 5% sodium hexametaphosphate in de-ionised water. Grain size distributions between 0.02 and 2000 mm were determined by laser diffraction spectrometry using a Malvern Mastersizer 2000. Major element concentrations were measured on bulk sediments using a Perkin Elmer Optima 3300RL ICP-AES, calibrated using single and multi-element standard solutions. Sample preparation followed the wet-chemical extraction procedure outlined in Engstrom and Wright (1984) and was undertaken at 2 cm intervals.

A combination of AMS ^{14}C and OSL dating was used to constrain the chronologies of the sites and details are provided elsewhere (Parker *et al*., 2006; Preston *et al*., 2015) (Figs. 3 and 4). Calibration of radiocarbon dates was undertaken using the Intcal13 calibration curve (Reimer *et al*., 2013). Age-depth modelling was performed on the ^{14}C and OSL dates using the software package Bacon version 2.2 (Blaauw and Christen, 2011) with R version 3.1.2 (R Core Team, 2014) (Fig. 5). Bacon uses Bayesian statistics and Markov chain Monte Carlo (MCMC) methods to reconstruct sediment accumulation histories, and estimates sedimentation times (a cm^{-1}) and ages through a dated section. Sedimentation times were converted into sedimentation rates (measured in cm a^{-1}) by taking the reciprocal (i.e. 1/sedimentation time) (Fig. 6). The means of the MCMC-derived age-depth models and sedimentation rate estimates were used to calculate proxy flux rates (see below).

The mass accumulation rate (MAR) of sediment per sample at both sites was calculated following the method outlined in Street-Perrott *et al*. (2007) where MAR (g $cm^{-2}a^{-1}$) equals DBD

(g cm^{-3}) multiplied by the sedimentation rate (SR) (cm a^{-1}), which is related to the respective depth-age relationship. The flux of magnetic minerals was calculated as follows: FLUX = DBD x SR x MS. Geochemical flux values (Al, Fe, K, Si and Ti) are expressed as concentrations per unit weight of sediment and expressed in (mg $cm^{-2}a^{-1}$) and were calculated by multiplying the MAR by the concentration by weight (mg g^{-1}).

The data generated by the above measurements are used to reconstruct changing environmental conditions over time. Dry bulk density (DBD) is used to infer changing sediment properties, with high values indicative of higher minerogenic content. Organic matter (OM) values are primarily controlled by biological productivity, together with organic matter preservation (Meyers, 2003). Magnetic susceptibility (MS) is used to infer stability in the surrounding dune-fields, with values primarily controlled by the deposition of Fe-rich quartz during periods of dune remobilisation (Preston *et al*., 2012), and may in turn be linked to variations in vegetation cover, precipitation, sediment supply and/or wind strength (Tsoar, 2005; Yizhaq *et al*., 2009). Reduced sediment input from the catchment is also inferred by lower Al, K, Fe, Si and Ti values, which correspond to the abundance of quartz, feldspars and sheet silicates, all of which are common components of the dune sands in the northern Emirates (El-Sayed, 1999; Farrant *et al*., 2015). Low Na/Ti and high Al/(Ca + Na) values are used to infer lake lowering, aridity and input of aeolian material rich in Ti and Al.

RESULTS

The results from the multi-proxy analyses are shown in Figs. 7 and 8. The flux rates are reported using the same units in order to facilitate comparisons between the sites through time.

Awafi

The base of the Awafi sequence comprises homogeneous, fine sands (210 to 160 μm), with the deposition of laminated marls with intermittent fine sands dated to ~8.3 k cal a BP. Although initially high, DBD (1.23 g cm^{-3}) and MAR (0.18 g cm^{-2} a^{-1}) values steadily decline until ~8.2 k cal a BP after which a marked increase is observed in sediment mass accumulation rates (MAR) (rising from 0.08 to 0.28 g $cm^{-2}a^{-1}$). A peak in detrital input occurs at ~8.1 k cal a BP with increases in the Al, Fe, K, Si and Ti. Two distinct peaks (>700) are recorded in the Na/Ti data between ~7.9 and 7.8 k cal a BP before values fall abruptly. Detrital sediment input is low between ~7.6 and 6.4 k cal a BP and is associated with reduced sediment MAR, as well as low geochemical flux values. Sediments comprise laminated marls with very fine sands and silts (105 to 45 μm). Organic matter (OM) flux values are very low (~1 mg $cm^{-2}a^{-1}$) between ~7.5 and 6.4 k cal a BP.

Sediment MAR increases from ~6.4 k cal a BP, corresponding with a steady increase in DBD values between ~6.1 (0.46 g cm^{-3}) and 5.0 k cal a BP (1.07 g cm^{-3}). The MS and geochemical flux data all show increasing values from ~6.4 k cal a BP, corresponding with an abrupt increase in the sand component of the sediment. Organic matter (OM) flux shows increasing values between ~6.4 (0.68 mg $cm^{-2}a^{-1}$) and ~5.5 k cal a BP (8.02 mg $cm^{-2}a^{-1}$), before steadily declining to 2.57 mg $cm^{-2}a^{-1}$ at ~5.0 k cal a BP. Magnetic susceptibility flux values increase slowly between ~6.0 and 5.4 k cal a BP, after which a steep increase is observed to ~5.0 k cal a BP. Na/Ti values fall rapidly at ~6.0 k cal a BP from a peak of ~600. The period between ~5.0 and 4.3 k cal a BP is characterised by decreasing MS flux values, reduced DBD and lower sediment

MAR. Sediments comprise very fine calcareous sands and silts (115 to 55 μm), with an overall reduction in the sand component of the sediment. A distinct 10 cm band of very fine aeolian sands (100 μm) is OSL dated to 4.10 ka. This layer corresponds with peaks in DBD, MS flux (3.0×10^{-5} cm a^{-1}), and the sand fraction (~90%) although this is muted in the geochemical flux data.

Wahalah

The basal sediments at Wahalah are dated to ~9.4 k cal a BP and comprise homogeneous, fine to very fine sands (130 to 100 μm). At ~9.0 k cal a BP, the aeolian sands are replaced by laminated marls, with intermittent fine to very fine sands (220 to 100 μm). Sediment mass accumulation rates (MAR) are low at the base of the sequence (~0.05 g $cm^{-2}a^{-1}$) before values increase abruptly at ~8.4 k cal a BP, peaking at 0.13 g $cm^{-2}a^{-1}$ between ~8.2 and 8.0 k cal a BP. Magnetic susceptibility (MS) flux values are low until ~8.2 k cal a BP, when an increase to 0.12×10^{-5} cm a^{-1} is observed. Organic matter (OM) flux rates are initially low (0.42 mg cm^{-2} a^{-1}) before rising to 1.42 mg cm^{-2} between ~8.4 and 7.9 k cal a BP. The curves for Al, Fe, K, Si and Ti all show similar patterns with moderately high values between ~9.4 and 9.0 k cal a BP, followed by a shift to lower values between ~9.0 and 8.3 k cal a BP. Distinct peaks are observed in the DBD and geochemical flux data between ~8.2 and 8.0 k cal a BP. An inverse trend is observed in the Na/Ti data, with values falling from ~400 at ~8.4 k cal a BP to ~60 at ~8.0 k cal a BP. Between ~7.9 and 6.0 k cal a BP, reduced flux rates are indicated by lower MAR, with sediments comprising fine to very fine calcareous sands (170 to 90 μm). The sand component of the sediment is lowest at this time although values steadily increase from ~7.4 k cal a BP. Pulses of detrital sediment input are indicated by peaks in the MS, Al, Fe, K, Si, Ti flux data at ~7.6, ~7.2,

~6.8 and ~6.4 k cal a BP. Between ~7.8 and 7.6 k cal a BP Na/Ti values increase to ~370 before falling abruptly.

Between ~5.9 and 5.2 k cal a BP there is a marked increase in DBD (from 0.78 to 1.03 g cm^{-3}) coinciding with the deposition medium to fine aeolian sands (280 to 120 µm). Magnetic susceptibility flux values rise sharply from 0.09 to 0.31 x 10^{-5} cm a^{-1} at ~5.9 k cal a BP and remain high until ~5.2 k cal a BP. A peak (>90%) is observed in the sand component of the sediment at ~5.7 k cal a BP. Organic matter (OM) flux rates decline to ~0.27 mg cm^{-2} a^{-1} and remain low throughout the rest of the sequence. Al, Fe, K, Si and Ti flux values all rise abruptly, whilst Na/Ti values decline to ~30, the lowest of the sequence. After ~5.0 k cal a BP detrital sediment input is reduced, as denoted by the decreases in the MS, Al, Fe, K, Si, Ti flux values and the Al/(Ca+Na) data. Sediments comprise fine to very fine calcareous sands (190 to 120 µm). Between ~4.2 and 3.9 k cal a BP MS flux values increase from 0.07 to 0.31 x 10^{-5} cm a^{-1} with values then falling to 0.18 x 10^{-5} cm a^{-1} at ~3.8 k cal a BP. Al, Fe, K, Si and Ti flux values all increase at this time. Al/(Ca+Na) values increase from 0.11 to 0.45 between ~4.3 and 4.1 k cal a BP.

DISCUSSION

The records derived from the Awafi and Wahalah sediment sequences are well documented (Parker *et al*., 2004, 2006; Parker and Goudie, 2008; Preston *et al*., 2015) and have in turn raised important palaeoclimatic questions. Evidence from both sites supports the notion that aridity prevailed throughout SE Arabia during the LGM and earliest Holocene (Parker, 2010; Farrant *et al*., 2015), with a large number of OSL-dated dune records suggesting increased accumulation

and preservation between ~16 and 9 ka (Leighton *et al*., 2014) (Fig. 9). At Awafi, 7 m of dune accumulation occurred between 13.5 and 9.1 ka (1.60 m ka^{-1}) (Goudie *et al*., 2000) and at Wahalah two dune sequences yielded a net accumulation rate of 3 to 4 m ka^{-1} between 15.9 and 10.3 ka (Atkinson *et al*., 2011; Leighton *et al*., 2014). The accumulation of sands and the higher flux levels at the base of both sequences support the notion that the surrounding dunes were active prior to, and possibly during, the initial flooding of each basin. Marine records from the Arabian Sea (74KL) show increased Fe values (Fig. 9), implying that aeolian input from the Arabian interior was greater at this time (Sirocko *et al*., 1993).

The revised chronologies for Awafi and Wahalah reinforce the notion that the shift to humid conditions during the EHHP was not synchronous across the Peninsula. For example, lacustrine deposits date the onset of wetter conditions to ~11.0 k cal a BP at al-Hawa, Ramlat as-Sab'atayn, Yemen, (Lézine *et al*., 2007), 10.5 ka at Maqta, al-Hajar Mountains, Oman (Fuchs and Buerkert, 2008), and ~9.7 k cal a BP at Mundafan, Rub' al-Khali, Saudi Arabia (Rosenberg *et al*., 2011). Comparatively later ages are reported from lacustrine deposits at Tayma, An Nafud, Saudi Arabia (~9.2 k cal a BP) (Dinies *et al*., 2015) and in the Wahiba Sands, Oman (9.3 ka) (Radies *et al*., 2005). The refined chronologies presented here reveal a modified pattern of lake development at Wahalah from that described in Preston *et al*. (2015), with lacustrine sedimentation commencing ~500 years earlier at ~9.0 k cal a BP. Nonetheless, the new chronologies reaffirm the notion that both sites are out-of-step with many of the palaeoclimate records listed above. The reason for this is unclear, although as outlined in Preston *et al*. (2015), it does not necessarily imply a continuation of aridity in the region. The later onset of lacustrine sedimentation at Awafi (~8.3 k cal a BP) suggests that local factors, possibly related to changing

basin and catchment topography, were more conducive to lake formation at Wahalah during the early Holocene. In this respect it is noted that dune accumulation ceased somewhat later at Awafi (9.1 ka) compared to Wahalah (10.3 ka) (Goudie *et al*., 2000; Atkinson *et al*., 2011). We also acknowledge that there is some overlap between the revised ages at the 95% (2σ) confidence level. At Wahalah, the new age-depth model yields a mean age of 9009 cal a BP (8516 – 9804 cal a BP, 2σ) at 2.06 m. At Awafi, a mean age of 8305 cal a BP (8110 - 8577 cal a BP, 2σ) was derived at 2.50 m. These depths (2.06 and 2.50 m) mark the onset of marl sedimentation at each site. The possibility that lacustrine sedimentation commenced simultaneously at the two sites is thus statistically possible.

Palaeoclimate studies have until recently suggested that the timing of the transition to humid conditions during the EHHP varies according to latitude, reflecting the steady northward shift of the summer ITCZ and associated monsoon rainfall belt into Arabia during the early Holocene (Fleitmann *et al*., 2007) in response to orbital forcing (Parton *et al*., 2015). This argument is consistent with the Omani speleothem records, which suggest that monsoon rainfall reached southern Oman (Qunf Cave) by 10.6 ka and northern Oman (Hoti Cave) by 10.1 ka (Fleitmann *et al*., 2007) (Fig. 9). Despite the absence of speleothem evidence supporting the displacement of the summer ITCZ as far as 27°N (Rosenberg *et al*., 2013), isotopic analysis of early Holocene groundwater samples from the Liwa and Gachsaran aquifers, UAE (23 to 24°N) suggests a southerly moisture source (Wood, 2010). Indeed, recent palaeoclimate modelling highlights the potential importance of moisture derived from the African monsoon system during interglacial phases (Rosenberg *et al*., 2013; Jennings *et al*., 2015). These models estimate an annual precipitation level of between 300 and 600 mm in the study region at 130 ka (Fig 3, Jennings *et*

al., 2015). Furthermore, they suggest that moisture derived from both Indian and African monsoon systems reached the study area during the last interglacial, increasing precipitation between May and December (Jennings *et al*., 2015). The development of this precipitation regime between ~9.0 and 8.0 k cal a BP, when most palaeoclimate records suggest peak monsoon activity, may have triggered a threshold response in both lake systems. The contribution of MLW rainfall, particularly throughout northern Arabia where such systems are important today, also warrants further investigation (Preston *et al*., 2015) although the above palaeoclimate models suggest that rainfall from these systems was low in comparison to monsoon-derived sources during the last interglacial (Jennings *et al*., 2015).

Palaeoclimate records indicate maximum humidity throughout Arabia between 9.0 and 7.0 k cal a BP (Berger *et al*., 2012), a finding consistent with the evidence discussed here. At Wahalah, Preston *et al*. (2015) suggest the development of permanent lacustrine conditions between ~8.5 and 7.7 k cal a BP (revised chronology; ~9.0 – 7.6 k cal a BP) based on the microfaunal evidence from the site, whereas a peak in scrub woodland taxa (primarily *Acacia* and *Prosopis*) is recorded in the Awafi pollen data at this time (Parker *et al*., 2004). The evidence presented here suggests that the EHHP (~9.0 and 6.4 k cal a BP) was characterised by overall landscape stability, with the lower flux values suggested to reflect the stabilisation of dunes as conditions became wetter. Leighton *et al*. (2014) demonstrated that dune records from SE Arabia show an abrupt fall in net dune accumulation rates at this time (Fig. 9). During much of the EHHP, the potential for the Rub' al-Khali dune fields to supply sediment would have been limited owing to the wetter conditions, the stabilising vegetation cover (Parker *et al*., 2004), and the flooding of the Arabian Gulf basin (Lambeck, 1996). Despite this, both records reveal several short-lived

phases of increased detrital sediment flux, the most prominent of which is dated between ~8.3 and 7.9 k cal a BP. At Awafi, Parker *et al*. (2004) reported an increase in the C_4 vegetation component at this time, which was suggested to be a response to increased aridity (Parker *et al*., 2004). Although this event is recorded in the Wahalah DBD and concentration (ppm) geochemical data reported in Preston *et al*. (2015), it is not as pronounced as it appears in the new data, in particular the new MS flux data. These differences highlight the benefit of MAR and sediment flux data in identifying abrupt, short-term events that otherwise appear muted or are missed in sediment records owing to variable sedimentation rates or dilution effects. Abrupt climatic change around this time has been documented in the African Tropics (Street-Perrott and Perrott, 1990), the Near East (Bar-Matthews *et al*, 2003), the Arabian Sea (Gupta *et al*., 2003), and the Thar desert (Dixit *et al*., 2014a). Corresponding phases of reduced precipitation are also noted in the Omani speleothem $\delta^{18}O$ data (Fleitmann *et al*., 2007) (Fig. 9), supporting the notion that the event led to large amplitude hydrological changes. In SE Arabia we suggest that positive biophysical non-linear feedback led to a prolonged phase of increased aridity, loss of vegetation, increased wind strength or a combination of these factors. Pulses of increased detrital sediment flux are also observed at Wahalah at ~7.6, ~7.2, ~6.8 and ~6.4 k cal a BP, with the earliest event also observed at Awafi. These events were insufficient to initiate large-scale dune accumulation throughout SE Arabia (Leighton *et al*., 2014) (Fig. 9).

The termination of the EHHP is characterised by considerable temporal heterogeneity, with Arabian palaeoclimate records broadly divided into: (a) those that show a gradual decrease in rainfall from ~8.0 k cal a BP and (b) those that show a more abrupt change at ~6.0 k cal a BP (Rampelbergh *et al*., 2013). The records from this study fall into the latter category, with aridity

at both sites more sustained between ~6.4 and 5.0 k cal a BP than at any point during the EHHP. At Awafi a steady increase in detrital sediment flux is recorded from ~6.4 k cal a BP, corresponding with a change to reduced vegetation cover with a greater C_4 component (Parker *et al*., 2004). The increase in OM in the Awafi record between ~6.4 and 5.5 k cal a BP may reflect a shallowing of the water body to more marshy conditions, the input of organic matter derived from the erosion and deflation of early Holocene soil material into the basin or a combination of both. This phase of aridity peaked between ~5.2 and 5.0 k cal a BP. In contrast, at Wahalah a more abrupt change is observed, with peaks in DBD, MS, Al, Fe, K, Si and Ti flux values between ~5.9 and 5.2 k cal a BP. This coincides with a rapid phase of dune accumulation at the site, with 4 m of sand deposited between 5.9 and 5.2 ka (5.9 m ka^{-1}) (Atkinson *et al*., 2011). Leighton *et al*. (2014; p. 11) suggest that the increase in aeolian activity occurred (Fig. 9) following a 'breached threshold of sediment availability as moisture levels fell', with increasing sediment availability most likely due to the loss of vegetation. Marine records from the Gulf of Oman show a small peak in dolomite at ~5.1 k cal a BP as a consequence of increased terrigenous dust input from the Arabian interior (Cullen *et al*., 2000) (Fig. 9). The contrasting responses of the Awafi and Wahalah lake records suggest differential sensitivities to increasing aridity, with overall higher precipitation at the former site owing to its closer proximity to the mountain front.

The termination of the EHHP is widely linked to the steady southward movement of the summer ITCZ from ~8.0 k cal a BP in response to declining solar insolation (Fig. 9), a theory consistent with evidence from the Qunf Cave speleothem record (Fleitmann *et al*., 2007), as well as sedimentary cores from the Arabian Sea (Sirocko *et al*., 1993; Gupta *et al*., 2003), which show a

gradual trend towards dry conditions in the Arabian interior (Fig. 9). Whilst the lake records discussed in this paper show a more abrupt shift as they became disconnected from southerly summer rainfall during the mid-Holocene (Rampelbergh *et al*., 2013), the sediment archives from both sites reveal long-term changes from ~8.0 k cal a BP. At Wahalah, Preston *et al*. (2015) noted a decline in microfauna (e.g. ostracods and gastropods) at ~7.7 k cal a BP (new chronology; ~7.6 k cal a BP), possibly reflecting a shift from permanent to intermittent conditions at the site. At Awafi, Parker *et al*. (2004) documented a decline in woody vegetation and a small increase in xeric taxa at approximately the same time, broadly corresponding with the abrupt decline in the Na/Ti data from this study. It is thus possible that these changes mark the onset of a progressive decline in precipitation, with rainfall from southern sources reaching the region less frequently after ~8.0 k cal a BP until a threshold was crossed between ~6.4 and 5.9 k cal a BP, triggering a widespread landscape reconfiguration. This view is supported by the abrupt positive shift in the Hoti Cave $\delta^{18}O$ speleothem record at 6.3 ka, which is suggested to reflect a change from a southern (monsoon) to a northern (MLW) moisture source (Fleitmann *et al*., 2007). Despite this, we propose that the termination of the EHHP cannot solely be explained by a simple south – north precipitation gradient. Indeed, the estimated position of the summer ITCZ during the early to mid-Holocene varies between studies (Pietsch and Kühn, 2012), with records from eastern areas of the Peninsula (e.g. Parker *et al*., 2006; Fleitmann *et al*., 2007; Fuchs and Buerkert, 2008) generally suggesting a more northerly position later into the Holocene than those in the southwest (e.g. Pietsch and Kühn, 2012). This is further complicated by the potential influence of the African monsoon system, with an associated west – east precipitation gradient across Arabia (Jennings *et al*., 2015). The importance of orography must also be considered, with records from or close to mountainous regions benefitting from increased

precipitation and runoff. Indeed, the orographic effects of the al-Hajar Mountains have already been discussed and are evident in palaeoclimate models (Jennings *et al*., 2015). A final consideration is the role played by MLW systems at the end of the EHHP. A shift to higher $\delta^{18}O$ values in the Soreq Cave speleothem record (Bar-Matthews *et al*., 2003) and termination of the Hoti Cave record at 5.3 ka (Fleitmann *et al*., 2007) (Fig. 9) suggests a decline in this source of moisture during the mid-Holocene although the evolution of MLW rainfall (e.g. spatial extension) is not yet precisely defined (Berger *et al*., 2012).

Following the termination of the EHHP (~6.4 to 5.0 k cal a BP), both records show a reduction in detrital sediment flux between ~5.0 and 4.3 k cal a BP, corresponding with lower net accumulation rates throughout the northeastern UAE (Leighton *et al*., 2014) (Fig. 9). These changes have previously been suggested to represent a short-term humid phase, the mid-Holocene humid period (MHHP), during which both the Awafi and Wahalah basins contained shallow, intermittent waters (Parker *et al*., 2006; Preston *et al*., 2015). An increase in the C_4 vegetation (Parker *et al*., 2004) suggests that the prevailing climate between ~5.0 and 4.3 k cal a BP was drier than between ~9.0 and 6.4 k cal a BP. Based on the current palaeoclimate evidence, it remains unclear whether this was a regional or more localised phase. Indeed, aside from the lake records presented here, very few archives show humid conditions at this time and those that do are predominately located in the southwest of the Peninsula (e.g. soil development in the Dhamar Highlands) where rainfall remains higher today (Davies *et al*., 2006). Since no palaeomonsoon records show a re-advance of the ITCZ at this time, we propose these humid conditions were primarily driven by increased MLW precipitation. An increase in MLW precipitation at this time is not consistent with the hiatus in the Hoti Cave speleothem record

between 5.3 and 2.6 ka (Fleitmann *et al*., 2007) although a brief humid phase is recorded in the Soreq Cave speleothem record between 4.8 and 4.7 ka (Bar-Matthews and Ayalon, 2011). Determining the spatial extent of the MHHP is challenging owing to possible removal of sediments by erosional processes during the predominately arid conditions that have prevailed since the mid-Holocene, with evidence only preserved at sites protected from the effects of such processes (e.g. archives at higher elevations, in areas of high groundwater, etc.). The deposition of aeolian sand in the Awafi lake basin at 4.10 ka marks the total desiccation of the water body. A corresponding increase in detrital sediment flux is recorded at Wahalah, with a peak in activity dated between ~4.2 and 3.9 k cal a BP. At Al Ain, UAE, 7 m of dune accumulation occurred between 4.4 and 4.1 ka giving a net accumulation rate of 26 m ka^{-1} (Atkinson *et al*., 2011). This event has a global signature and is identified in palaeoclimate records throughout Arabia (Arz *et al*., 2006; Berger *et al*., 2012), as well as other areas influenced by the monsoon system (Street-Perrott and Perrott, 1990; Cullen *et al*., 2000; Staubwasser *et al*., 2003; Tierney and deMenocal, 2013; Dixit *et al*., 2014b) (Fig. 9).

Previous studies have highlighted a potential link between abrupt events identified in the Awafi and Wahalah sediment records and Bond Events (Bond *et al*., 1997) driven by reduced sea surface temperatures (SST) in the North Atlantic (Parker *et al*., 2006; Preston *et al*., 2015). Indeed, the abrupt increases in detrital sediment flux identified in this study between ~8.3 and 7.9 k cal a BP, at 5.9 k cal a BP, and between ~ 4.3 and 3.9 k cal a BP fall within periods of rapid climate change identified by Mayewski *et al*. (2004), which were typically characterised by reduced temperatures at high latitudes, increased aridity throughout the lower latitudes, and major changes to atmospheric circulation, including reduced monsoon intensity. We propose that

in SE Arabia these events drove threshold changes across the landscape, with resultant fluctuations in lake levels, sediment availability and flux rates.

Conclusions

Sediment flux data from SE Arabia show the sensitivity of high-resolution terrestrial records from this region. The revised chronologies presented in this paper reaffirm the notion that the Awafi and Wahalah records are out-of-step with other palaeoclimate records from Arabia. This may partly reflect the gradual northwards migration of the summer ITCZ and associated Indian monsoon rains during the EHHP (~9.0 to 6.4 k cal a BP) although the contribution of moisture derived from the African monsoon system as well as MLW at this time remains uncertain and warrants further investigation. Despite maximum lake expansion, vegetation cover, and overall landscape stability during the EHHP, several pulses of increased detrital sediment input are recorded at the study sites, the most prominent dates between ~8.3 and 7.9 k cal a BP, and are suggested to reflect short-lived phases of increased aridity. The termination of the EHHP is linked to southwards migration of the summer ITCZ to its present position from ~8.0 k cal a BP. The abrupt changes observed at both sites between ~6.4 and 5.9 k cal a BP may reflect a threshold response of the landscape to this long-term decrease in precipitation, with aridity peaking between ~5.2 and 5.0 k cal a BP. This was followed by a period of reduced detrital sediment flux during the MHHP (~5.0 to 4.3 k cal a BP), which is suggested to reflect a brief return to more humid conditions. The spatial extent of the proposed increase in moisture remains unclear. The termination of the MHHP is marked by an abrupt increase in detrital sediment flux in both records between ~4.3 to 3.9 k cal a BP. This event, as well as the suggested increases in aridity between ~8.3 and 7.9 and at ~5.9 k cal a BP, is coeval with phases of rapid global climate

change, which appear to have driven non-linear changes throughout the SE Arabian landscape characterised by dune reactivation, lake lowering and vegetation loss.

ACKNOWLEDGEMENTS

The underlying concepts for this research were heavily influenced by the work of Alayne Street-Perrott and the seeds sown whilst AGP was a research student under her supervision. We thank Christian Velde and Imke Moellering, Department of Antiquities, Government of Ras' al-Khaimah, for permission to work in the area and for providing logistical support. PEJ is funded by NERC grant NE/KOO5294/1. Finally, the authors wish to thank the two anonymous reviewers and the guest editor for their constructive feedback on earlier drafts of this manuscript.

REFERENCES

Alsharhan AS, Rizk ZA, Nairn AEM, Bakhit DW, Alhajari SA. 2001. *Hydrology of an Arid Region: The Arabian Gulf and Adjoining Areas*. Elsevier Science B.V: Amsterdam; 206.

Arz HW, Lamy F, Pätzold J. 2006. A pronounced dry event recorded around 4.2 kyr in brine sediments from the Northern Red Sea. *Quaternary Research* **66**: 432–441.

Atkinson OA, Thomas DSG, Goudie AS, Bailey RM. 2011. Late Quaternary chronology of major dune ridge development in the northeast Rub' al-Khali, United Arab Emirates. *Quaternary Research* **76**: 93–105.

Atkinson OA, Thomas DS, Goudie AS, Parker AG. 2012. Holocene development of multiple dune generations in the northeast Rub'al-Khali, United Arab Emirates. *The Holocene* **22**: 179–189.

Barker P, Street-Perrott FA, Leng MJ, Greenwood PB, Swain DL, Perrott RA, Telford RJ, Ficken KJ. 2001. A 14,000-year oxygen isotope record from diatom silica in two alpine lakes on Mt. Kenya. *Science* **292**: 2307–2310.

Bar-Matthews M, Ayalon A. 2011. Mid-Holocene climate variations revealed by high-resolution speleothem records from Soreq Cave, Israel and their correlation with cultural changes. *The Holocene* **21:** 163–171.

Bar-Matthews M, Ayalon A, Gilmour M, Matthews A, Hawkesworth CJ, 2003. Sea-land oxygen isotope relationships from planktonic foraminifera and speleothems in the eastern Mediterranean region and their implication for paleorainfall during interglacial intervals: *Geochimica et Cosmochimica Acta* **67**: 3181–3199.

Berger A, Loutre M F. 1991. Insolation values for the climate of the last 10 million years. *Quaternary Science Reviews* **10**: 297–317.

Berger J-F, Bravard J-P, Purdue L, Benoist A, Mouton M, Braemer F. 2012. Rivers of the Hadramawt watershed (Yemen) during the Holocene: clues of late functioning. *Quaternary International* **266**: 142–161.

Blaauw M. 2010. Methods and code for 'classical' age-modelling of radiocarbon sequences. *Quaternary Geochronology* **5:** 510–518.

Blaauw M, Christen JA. 2011. Flexible paleoclimate age-depth models using an autoregressive gamma process. *Bayesian Analysis* **6**: 457–474.

Bond G, Showers W, Cheseby M, Lotti R, Almasi P, deMenocal P, Priore P, Cullen H, Hadjas I, Bonani G. 1997. A pervasive millennial-scale cycle in North Atlantic Holocene and glacial climates. *Science* **278**: 1257–1266.

Cockerton HE, Holmes JA, Street-Perrott FA, Ficken KJ. 2014. Holocene dust records from the West African Sahel and their implications for changes in climate and land surface conditions. *Journal of Geophysical Research – Atmospheres* **119**: 8684–8694.

Cullen HM, DeMenocal PB, Hemming S, Hemming G, Brown FH, Guilderson T, Sirocko F. 2000. Climate change and the collapse of the Akkadian empire. *Geology* **28**: 379–382.

Davies CP. 2006. Holocene palaeoclimates of Southern Arabia from lacustrine deposits of the Dhamar highlands, Yemen. *Quaternary Research* **66:** 454–464.

Dearing J. 1999. Magnetic Susceptibility. In *Environmental Magnetism: a Practical Guide*, Walden J, Oldfield F, Smith J (eds). Quaternary Research Association: London; 35–63.

deMenocal PM, Ortiz J, Guilderson T, Adkins J, Sarnthein M, Baker L, Yarusinsky M. 2000. Abrupt onset and termination of the African Humid Period: Rapid climate responses to gradual insolation forcing. *Quaternary Science Reviews* **19:** 347–361.

Dinies M, Plessen B, Neef R, Kürschner H. 2015. When the desert was green: Grassland expansion during the early Holocene in northwestern Arabia. *Quaternary International* **382**: 293–302.

Dixit Y, Hodell DA, Sinha R, Petrie CA. 2014a. Abrupt weakening of the Indian summer monsoon at 8.2 kyr BP. *Earth and Planetary Science Letters* **391**: 16–23.

Dixit Y, Hodell DA, Petrie CA. 2014b. Abrupt weakening of the summer monsoon in northwest India ~4100 yr ago. *Geology* **43:** 339–342.

Engstrom W, Wright Jr HE. 1984. Chemical stratigraphy of lake sediments as a record of environmental change. In *Lake Sediments and Environmental History,* Haworth EY, Lund JWD (eds). Leicester University Press: Leicester; 11–67.

El-Sayed MI. 1999. Sedimentological characteristics and morphology of the aeolian sand dunes in the eastern part of the UAE: a case study from Ar Rub' Al Khali. *Sedimentary Geology* **123**: 219–238.

Farrant AR, Ellison RA, Thomas RJ, Pharaoh TC, Newell AJ, Goodenough KM, Lee JR, Knox R. 2012. The Geology and Geophysics of the United Arab Emirates. In *Volume 6: Geology of the western and central United Arab Emirates*. British Geological Survey: Keyworth, Nottingham.

Farrant AR, Duller GA, Parker AG, Roberts HM, Parton A, Knox RW, Bide T. 2015. Developing a framework of Quaternary dune accumulation in the northern Rub' al-Khali, Arabia. *Quaternary International* **382**: 132–144.

Ficken KJ, Wooller MJ, Swain DL, Street-Perrott FA, Eglinton G. 2002. Reconstruction of a subalpine grass-dominated ecosystem, Lake Rutundu, Mount Kenya: a novel multi-proxy approach. *Palaeogeography, Palaeoclimatology, Palaeoecology* **177**: 137–149.

Fisher M, Membery D. 1998. Climate. In *Vegetation of the Arabian Peninsula,* Ghazanfar SA, Fisher M (eds). Kluwer Academic Publications: Dordrecht; 5–38.

Fleitmann D, Burns SJ, Mangini A, Mudelsee M, Kramers J, Villa I, Neff U, Al-Subbary A, Buettner A, Hipper D, Matter A . 2007. Holocene ITCZ and Indian monsoon dynamics recorded in stalagmites from Oman and Yemen (Socotra). *Quaternary Science Reviews* **26**: 170–188.

Fuchs M, Buerkert A. 2008. A 20 ka sediment record from the Hajar Mountain range, N. Oman, and its implications for detecting arid – humid periods of the southeastern Arabian Peninsula. *Earth and Planetary Science Letters* **265:** 546–558.

598 Glennie KW, Singhvi AK. 2002. Event stratigraphy, palaeoenvironment and chronology of SE
599 Arabian deserts. *Quaternary Science Reviews* **21:** 853–869.
600
601 Goudie AS, Colls A, Stokes S, Parker AG, White K, Al-Farraj A. 2000. Latest Pleistocene dune
602 construction at the north-eastern edge of the Rub al Khali, United Arab Emirates. *Sedimentology*
603 **47**: 1011–1021.
604
605 Gupta AK, Anderson DM, Overpeck JT. 2003. Abrupt changes in the Asian southwest monsoon
606 during the Holocene and their links to the North Atlantic Ocean. *Nature* **421**: 354–356.
607
608 Heiri O, Lotter AF, Lemcke G. 2001. Loss on ignition as a method for estimating organic and
609 carbonate content in sediments: reproducibility and comparability of results. *Journal of*
610 *Paleolimnology* **25:** 101–110.
611
612 Jennings R, Singarayer J, Stone E, Krebs-Kanzow U, Khon V, Nisancioglu KH, Pfeffer M,
613 Zhang X, Parker AG, Parton A, Groucott H, White TS, Drake N, Petraglia MD. 2015. The
614 greening of Arabia: an ensemble of climate model simulations infers multiple opportunities for
615 human occupation of the Arabian Peninsula during the Late Pleistocene. *Quaternary*
616 *International* **382**: 181–199.
617
618 Kutzbach JE, Street-Perrott FA. 1985. Milkankovitch forcing of fluctuations in the level of
619 tropical lakes from 18 to 0 BP. *Nature* **317:** 130–134.
620

Lambeck K. 1996. Shoreline reconstructions for the Persian Gulf since the last glacial maximum. *Earth and Planetary Science Letters* **142**: 43–57.

Leighton CL, Bailey RM, Thomas DSG. 2014. Interpreting and modelling late Quaternary dune accumulation in the southern Arabian Peninsula. *Quaternary Science Reviews* **102**: 1–13.

Lézine AM, Tiercelin JJ, Robert C, Saliège JF, Cleuziou S, Inizan ML, Braemer F. 2007. Centennial to millennial-scale variability of the Indian monsoon during the early Holocene from a sediment, pollen and isotope record from the desert of Yemen. *Palaeogeography, Palaeoclimatology, Palaeoecology* **243:** 235–249.

Mayewski PA, Rohling EE, Stager JC, Karlen W, Maascha KA, Meekler LD, Meyerson EA, Gasse G, van Kreveld S, Holmgren K, Lee-Thorp J, Rosqvist G, Rack F, Staubwasser M, Schneider RR, Steig EJ. 2004. Holocene climate variability. *Quaternary Research* **62:** 243–255.

Meyers PA. 2003. Applications of organic geochemistry to palaeolimnological reconstructions: a summary of examples from the Laurentian Great Lakes. *Organic Geochemistry* **34:** 261–289.

Neff U, Burns SJ, Mangini A, Mudelsee M, Fleitmann D, Matter A. 2001. Strong coherence between solar variability and the monsoon in Oman between 9 and 6 kyr ago. *Nature* **411**: 290–293.

643 Parker AG. 1995. *Late Quaternary environmental change in the Upper Thames Basin, central-*
644 *southern England.* DPhil thesis. University of Oxford, Oxford; 67–68.
645
646 Parker AG. 2010. Pleistocene climate change in Arabia: developing a framework for hominin
647 dispersal over the last 350 ka. In *The evolution of human populations in Arabia,* Petraglia M,
648 Rose J. (eds). Springer: Netherlands; 39–49.
649
650 Parker AG, Goudie AS. 2008. Geomorphological and palaeoenvironmental investigations in the
651 southeastern Arabian Gulf region and the implication for the archaeology of the region.
652 *Geomorphology* **101**: 458–470.
653
654 Parker AG, Eckersley L, Smith MM, Goudie AS, Stokes S, White K, Hodson MJ. 2004.
655 Holocene vegetation dynamics in the northeastern Rub' al Khali desert, Arabian Peninsula - a
656 pollen, phytolith and carbon isotope study. *Journal of Quaternary Science* **19**: 665–676.
657
658 Parker AG, Goudie AS, Stokes S, White K, Hodson MJ, Manning M, Kennet D. 2006. A record
659 of Holocene climate change from lake geochemical analyses in southeastern Arabia. *Quaternary*
660 *Research* **66**: 465–476.
661
662 Parton A, White TS, Parker AG, Breeze PS, Jennings R, Groucutt HS, Petraglia MD. 2015.
663 Orbital-scale climate variability in Arabia as a potential motor for human dispersals. *Quaternary*
664 *International* **382**: 82–97.
665

Pietsch D, Kühn P. 2012. Early Holocene paleosols at the southwestern Ramlat As-Sab'atayn desert margin: New climate proxies for southern Arabia. *Palaeogeography, Palaeoclimatology, Palaeoecology* **365–366:** 154–165.

Preston GW, Parker AG, Walkington H, Leng MJ, Hodson MJ. 2012. From nomadic herder-hunters to sedentary farmers: the relationship between climate change and ancient subsistence strategies in south-eastern Arabia. *Journal of Arid Environments* **86**: 122–130.

Preston GW, Thomas DSG, Goudie AS, Atkinson OA, Leng MJ, Hodson MJ, Walkington H, Charpentier V, Mery S, Biogi F, Parker AG. 2015. A multi-proxy analysis of the Holocene humid phase from the United Arab Emirates and its implications for southeast Arabia's Neolithic populations. *Quaternary International* **382**: 277–292.

Preusser F. 2009. Chronology of the impact of Quaternary climate change on continental environments in the Arabian Peninsula. *Comptes Rendus Geoscience* **341**: 621–632.

Preusser F, Radies D, Matter A. 2002. A 160,000-year record of dune development and atmospheric circulation in southern Arabia. *Science* **296**: 2018–2020.

Radies D, Hasiots ST, Preusser F, Neubert E, Matter A. 2005. Paleoclimatic significance of early Holocene faunal assemblages in wet interdune deposits of the Wahiba Sand Sea, Sultanate of Oman. *Journal of Arid Environments* **62:**109–125.

R Core Team. 2014. *R: A language and environment for statistical computing*. R Foundation for Statistical Computing: Vienna, Austria. Available at: http://www.R-project.org/.

Rampelbergh MV, Fleitmann D, Verheyden S, Cheng H, Edwards L, Geest PD, Vleeschouwer DD, Burns SJ, Matter A, Claeys P, Keppens E. 2013. Mid- to late Holocene Indian Ocean Monsoon variability recorded in four speleothems from Socotra Island, Yemen. *Quaternary Science Reviews* **65:** 129–142.

Reimer PJ, Bard E, Bayliss A, Beck, JW, Blackwell PG, Bronk Ramsey C, Buck CE, Cheng H, Edwards RL, Friedrich M, Grootes PM, Guilderson TP, Haflidason H, Hajda I, Hatté C, Heaton TJ, Hoffmann DL, Hogg AG, Hughen KA, Kaiser KF, Kromer B, Manning SW, Niu M, Reimer RW, Richards DA, Scott EM, Southon JR, Staff RA, Turney CSM, van der Plicht J. 2013. IntCal13 and Marine13 radiocarbon age calibration curves 0-50,000 years cal BP. *Radiocarbon* **55**: 1869–1887.

Rosenberg TM, Preusser F, Fleitmann D, Schwalb A, Penkman K, Schmid TW, Al-Shanti MA, Kadi K, Matter A. 2011. Humid periods in southern Arabia: windows of opportunity for modern human dispersal. *Geology* **39**: 1115–1118.

Rosenberg TM, Preusser F, Risberg J, Plikk A, Kadi KA, Matter A, Fleitmann D. 2013. Middle and Late Pleistocene humid periods recorded in palaeolake deposits of the Nafud desert, Saudi Arabia. *Quaternary Science Reviews* **70:** 109–123.

Shanahan TM, McKay NP, Hughen KA, Overpeck JT. 2015. The time-transgressive termination of the African Humid Period. *Nature Geoscience* **8:** 140–144.

Sirocko F, Sarnthein M, Erlenkeuser H, Lange H, Arnold M, Duplessy JC. 1993. Century-scale events in monsoonal climate over the past 24,000 years. *Nature* **364**: 322–324.

Staubwasser M, Sirocko F, Grootes PM, Segl M. 2003 Climate change at the 4.2 ka BP termination of the Indus valley civilisation and Holocene Asian monsoon variability. *Geophysical Research Letters* **30:** 1425–1428.

Stokes S, Bray HE. 2005. Late Pleistocene eolian history of the Liwa region, Arabian Peninsula. *Geological Society of America Bulletin* **117**: 1466–1480.

Street FA, Grove AT. 1976. Environmental and climatic implications of late Quaternary lake-level fluctuations in Africa. *Nature* **261**: 385–390.

Street FA, Grove AT. 1979. Global maps of lake-level fluctuations since 30,000 yr BP. *Quaternary Research* **12**: 83–118.

Street-Perrott FA, Harrison SP. 1984. Temporal variations in lake levels since 30,000 yr BP—an index of the global hydrological cycle. In *Climate Processes and Climate Sensitivity*, Hansen JE, Takahashi T (eds). American Geophysical Union: Washington, D.C; 118–129.

Street-Perrott FA, Harrison SP. 1985. Lake Level and Climate Reconstructions. In *Paleoclimate Analysis and Modeling,* Hecht AD (ed). John Wiley and Sons: New York; 291–340.

Street-Perrott FA, Perrott RA. 1990. Abrupt climate fluctuation in the tropics: the influence of Atlantic Ocean circulation. *Nature* **343**: 607–612.

Street-Perrott FA, Perrott RA. 1993. Holocene vegetation, lake levels and climate of Africa. Global climates since the last glacial maximum. In *Global Climates since the Last Glacial Maximum,* Wright, HE (ed). University of Minnesota Press: Minneapolis; 318–356.

Street-Perrott FA, Marchand DS, Roberts N, Harisson SP. 1989. *Global Lake-Level Variations from 18,000 to 0 Years Ago: A Paleoclimatic Analysis*. U.S. Department of Energy Technical Report 46, Washington, D.C. 20545.

Street-Perrott FA, Barker PA, Swain DL, Ficken KJ, Wooller MJ, Olago DO, Huang Y. 2007. Late Quaternary changes in ecosystems and carbon cycling on Mt. Kenya, East Africa: a landscape-ecological perspective based on multi-proxy lake-sediment influxes. *Quaternary Science Reviews* **26**: 1838–1860.

Telford RJ, Heegaard E, Birks HJB. 2004. All age-depth models are wrong: but how badly? *Quaternary Science Reviews* **23**: pp 1–5.

Thomas DSG, Burrough SL. 2012. Interpreting geoproxies of late Quaternary climate change in African drylands: implications for understanding environmental change and early human behaviour. *Quaternary International* **253**: 5–17.

Thomas DS, Burrough SL, Parker AG. 2012. Extreme events as drivers of early human behaviour in Africa? The case for variability, not catastrophic drought. *Journal of Quaternary Science* **27**: 7–12.

Tierney JE, deMenocal PB. 2013. Abrupt shifts in Horn of Africa hydroclimate since the Last Glacial Maximum. *Science* **342**: 843–846.

Tsoar H. 2005. Sand dunes mobility and stability in relation to climate. *Physica A: Statistical Mechanics and its Applications* **357:** 50–56.

White K, Goudie AS, Parker AG, Al-Farraj A. 2001. Mapping the geochemistry of the Northern Rub Al Khali using multispectral remote sensing techniques. *Earth Surface Processes and Landforms* **26**: 735**–**748.

Wood W. 2010. Source of paleo-groundwater in the Emirate of Abu Dhabi, United Arab Emirates: Evidence from unusual oxygen and deuterium isotope data. *Hydrogeology Journal* **19:** 155–161.

Yizhaq H, Ashkenazy Y, Tsoar H. 2009. Sand dune dynamics and climate change: a modelling approach. *Journal of Geophysical Research* **114** F01023: DOI: 10.1029/2008JF001138.

Yu G, Harrison SP. 1996. An evaluation of the simulated water balance of Eurasia and northern Africa at 6000 y BP using lake status data. *Climate Dynamics* **12:** 723–735.

FIGURE CAPTIONS

Figure 1: Map of the Arabian Peninsula showing the location of Awafi palaeolake (25° 42' 57" N, 57° 55' 57" E; 2 km^2), Wahalah palaeolake (25° 38' 48" N, 55° 47' 26" E; 2.4 km^2) and other key sites mentioned in the text. The relative atmospheric circulation patterns associated with the modern climate systems are shown. The dotted line indicates the approximate position of the Intertropical Convergence Zone (ITCZ) during the summer.

Figure 2: Satellite image showing the geomorphological setting of the northern UAE and the locations of the Awafi and Wahalah palaeolake basins. The solid lines represent the axes of the region's mega-linear dune ridges. The dotted lines show the distribution of alluvial fan deposits. Source of satellite image: Google Earth.

Figure 3: The Awafi sediment section showing the main stratigraphic units and the calibrated and uncalibrated ages.

Figure 4: The Wahalah sediment section showing the main stratigraphic units and the calibrated and uncalibrated ages.

Figure 5: Age-depth plots for (a) Wahalah and (b) Awafi. Blue symbols (on-line version) show the ^{14}C and OSL dates and their associated uncertainties. Solid lines are the mean MCMC-derived age-depth models and the dashed lines are the 95% confidence intervals.

Figure 6: Sedimentation rates for (a) Wahalah and (b) Awafi with ages derived from the mean age-depth model for each site (refer to Fig. 5). Solid lines are the mean MCMC-derived sedimentation rates and dashed lines are the 95% confidence intervals.

Figure 7: Sediment flux records for Awafi showing the key palaeoclimatic periods. The darker grey bands indicate periods of increased sediment flux and climatic aridity as discussed in the text.

Figure 8: Sediment flux records for Wahalah showing the key palaeoclimatic periods. The darker grey bands indicate periods of increased sediment flux and climatic aridity as discussed in the text.

Figure 9: Comparison of palaeoclimate records from Arabia and surrounding regions (refer to Fig. 1 for the location of each site): (1) Insolation at 30°N (Berger and Loutre, 1991), (2) Dune net accumulation rates from SE Arabia (Leighton *et al*., 2014), (3) Wahalah MS signal (10^{-5} cm a^{-1}), (4) Wahalah Ti flux record (mg $cm^{-2}a^{-1}$), (5) Awafi MS signal (10^{-5} cm a^{-1}), (6) Awafi Ti flux record (mg $cm^{-2}a^{-1}$), (7) $\delta^{18}O$ Soreq Cave speleothem record (Bar-Matthews *et al*., 2003), (8) $\delta^{18}O$ Hoti Cave speleothem record (‰) (Neff *et al*., 2001), (9) $\delta^{18}O$ Qunf Cave speleothem

record (‰) (Fleitmann *et al*., 2007), (10) Iron (ppm) record from core 74KL, Arabian Sea (Sirocko *et al*., 1993), (11) Dolomite (%) record from core M5-422, Gulf of Oman (Cullen *et al*., 2000), (12) *Globigerinoides ruber* $\delta^{18}O$ from core 63KA, Arabian Sea (Staubwasser *et al*., 2003), (13) δD_{wax} record from core P178-15P, Gulf of Aden (Tierney and deMenocal, 2013). The key palaeoclimatic periods discussed in the text are shown.

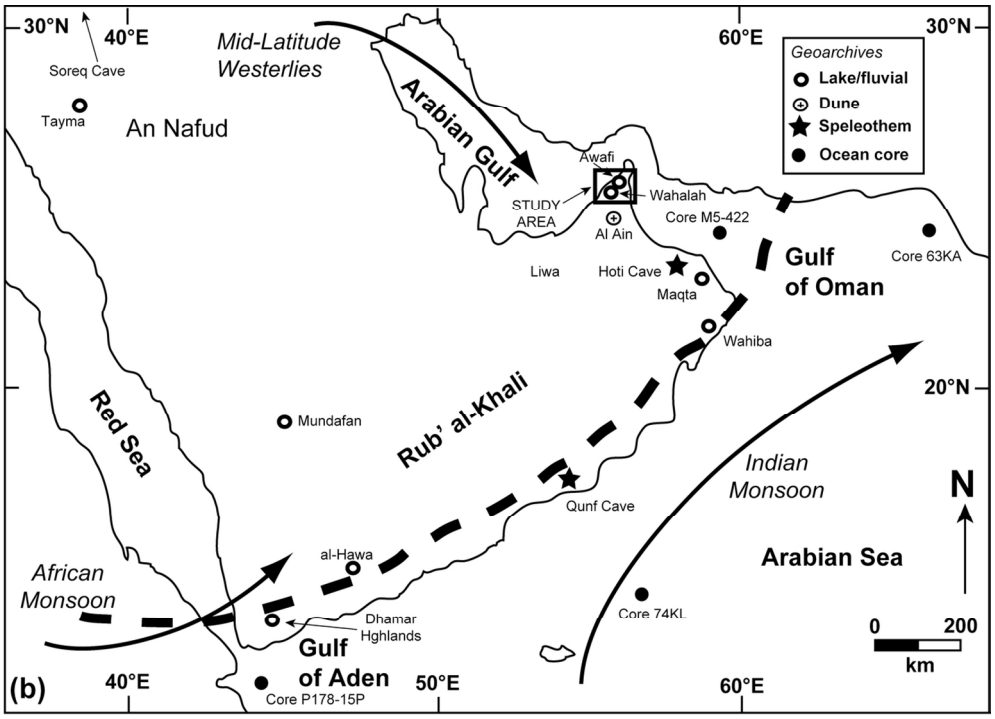

Figure 1: Map of the Arabian Peninsula showing the location of Awafi palaeolake (25° 42' 57" N, 57° 55' 57" E ; 2 km2), Wahalah palaeolake (25° 38' 48" N, 55° 47' 26" E ; 2.4 km2) and other key sites mentioned in the text. The relative atmospheric circulation patterns associated with the modern climate systems are shown. The dotted line indicates the approximate position of the Intertropical Convergence Zone (ITCZ) during the summer.
122x87mm (300 x 300 DPI)

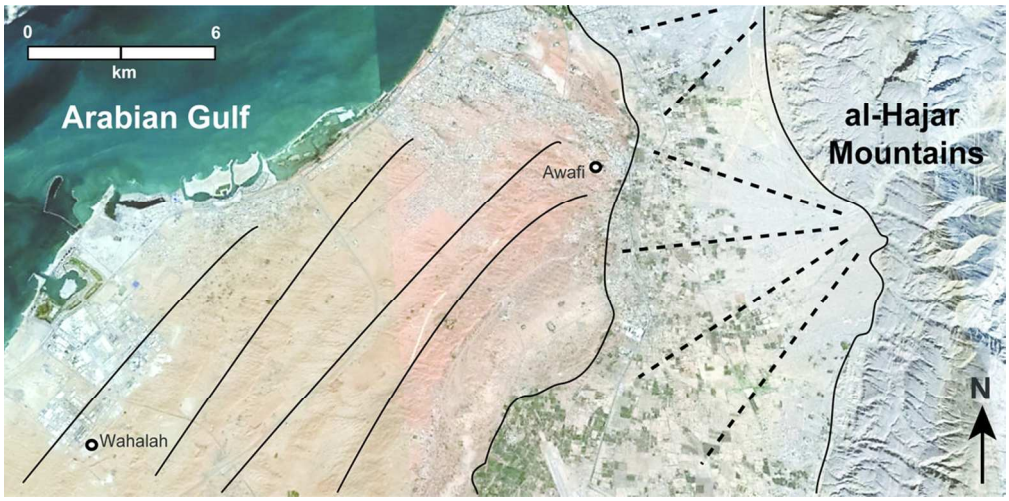

Figure 2: Satellite image showing the geomorphological setting of the northern UAE and the locations of the Awafi and Wahalah palaeolake basins. The solid lines represent the axes the region's mega-linear dune ridges. The dotted lines show the distribution of alluvial fan deposits. Source of satellite image: Google Earth.
99x49mm (300 x 300 DPI)

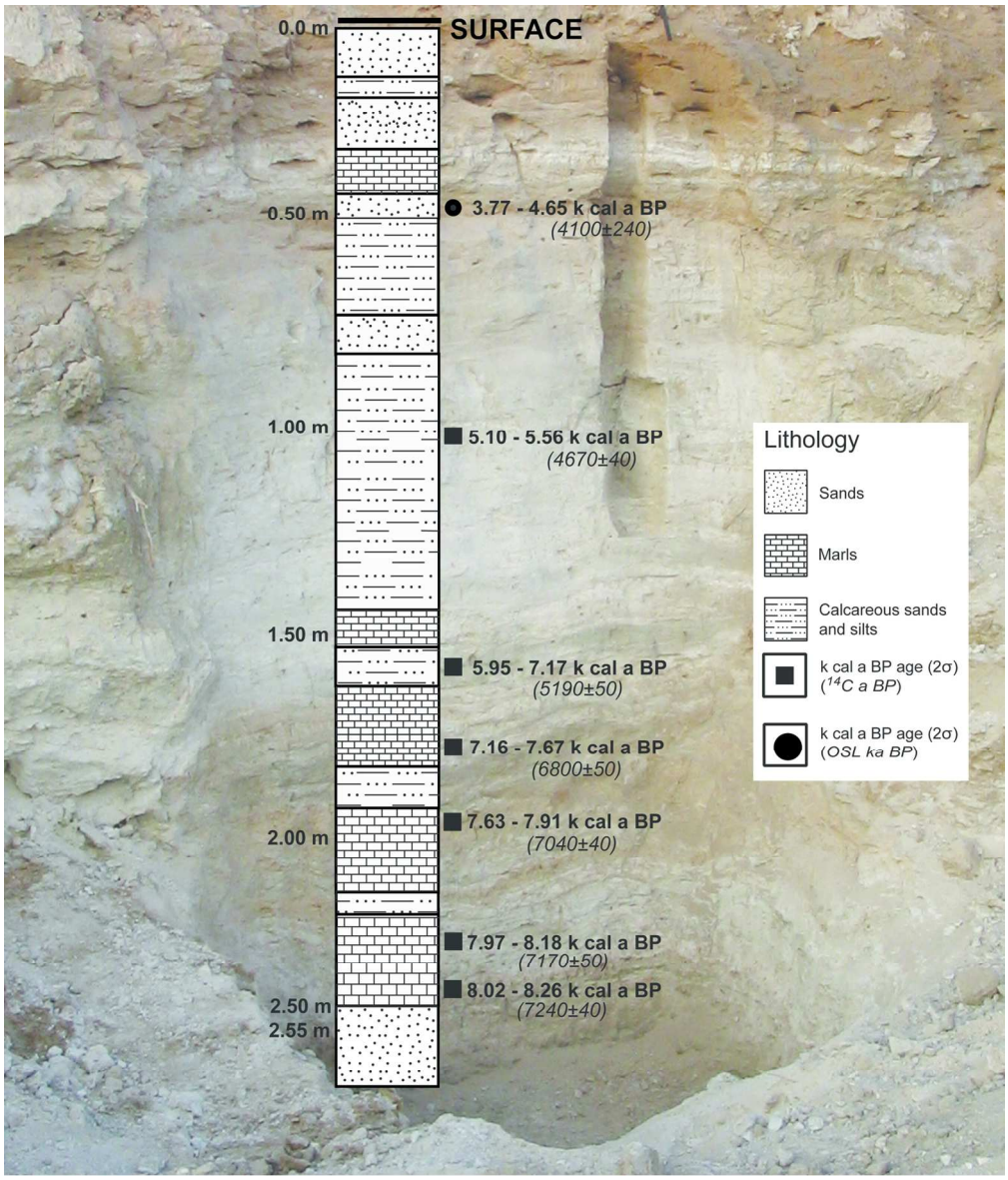

Figure 3: The Awafi sediment section showing the main stratigraphic units and the calibrated and uncalibrated ages.
145x169mm (300 x 300 DPI)

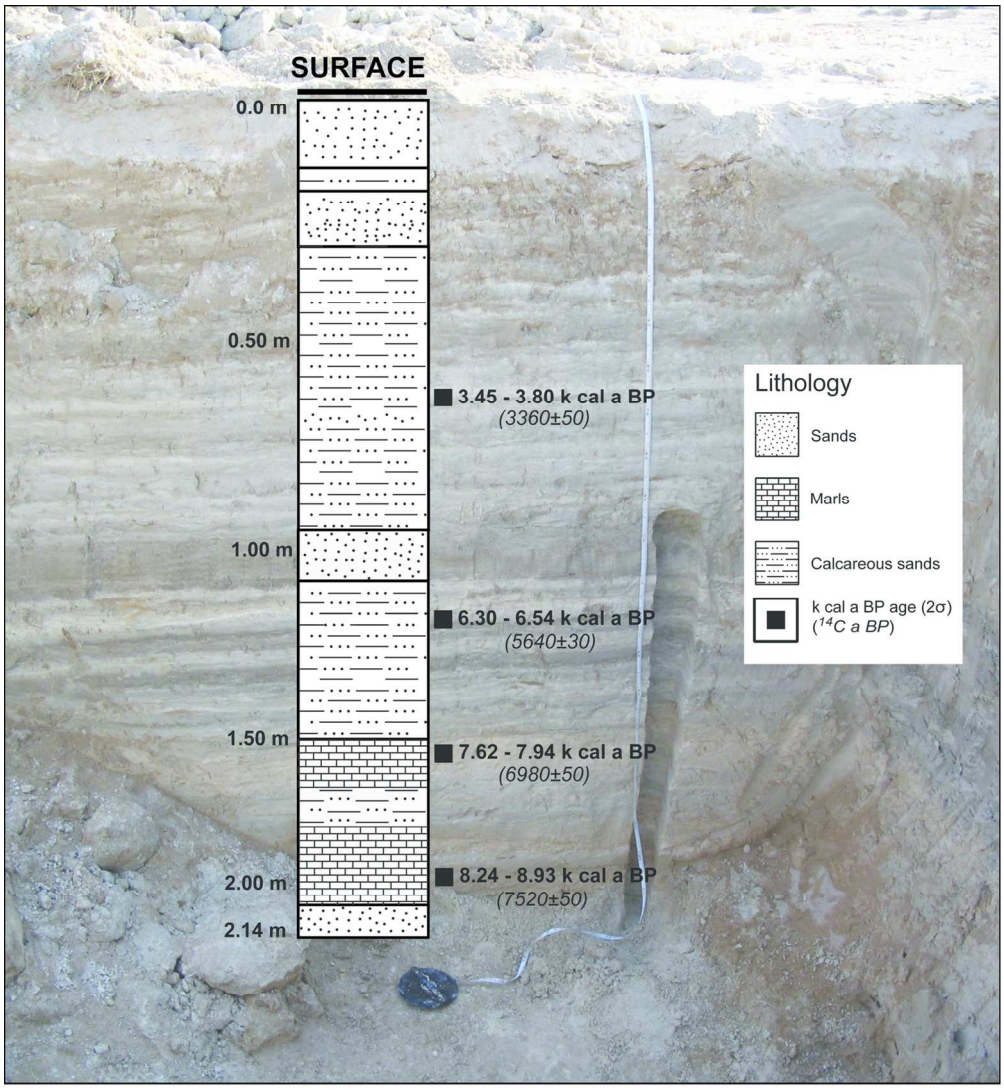

Figure 4: The Wahalah sediment section showing the main stratigraphic units and the calibrated and uncalibrated ages.
132x143mm (300 x 300 DPI)

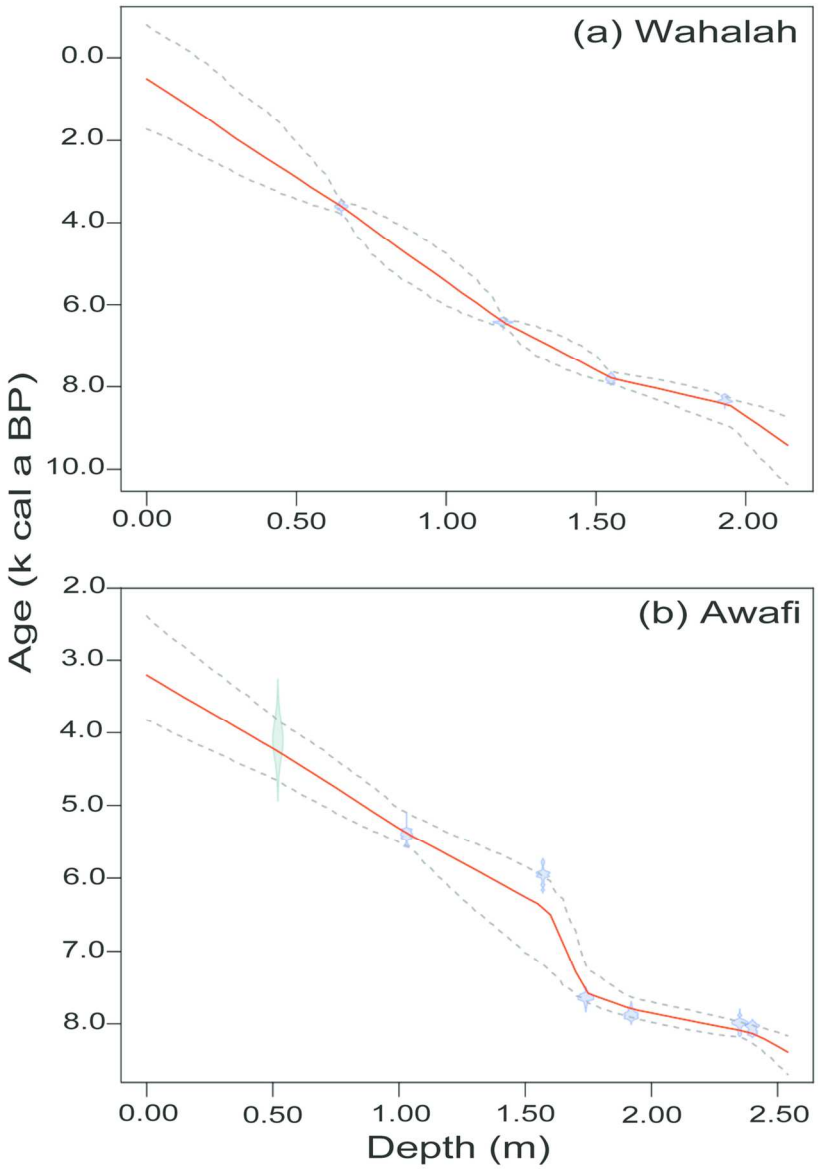

Figure 5: Age-depth plots for (a) Wahalah and (b) Awafi. Blue symbols (on-line version) show the 14C and OSL dates and their associated uncertainties. Solid lines are the mean MCMC-derived age-depth models and the dashed lines are the 95% confidence intervals.
110x156mm (300 x 300 DPI)

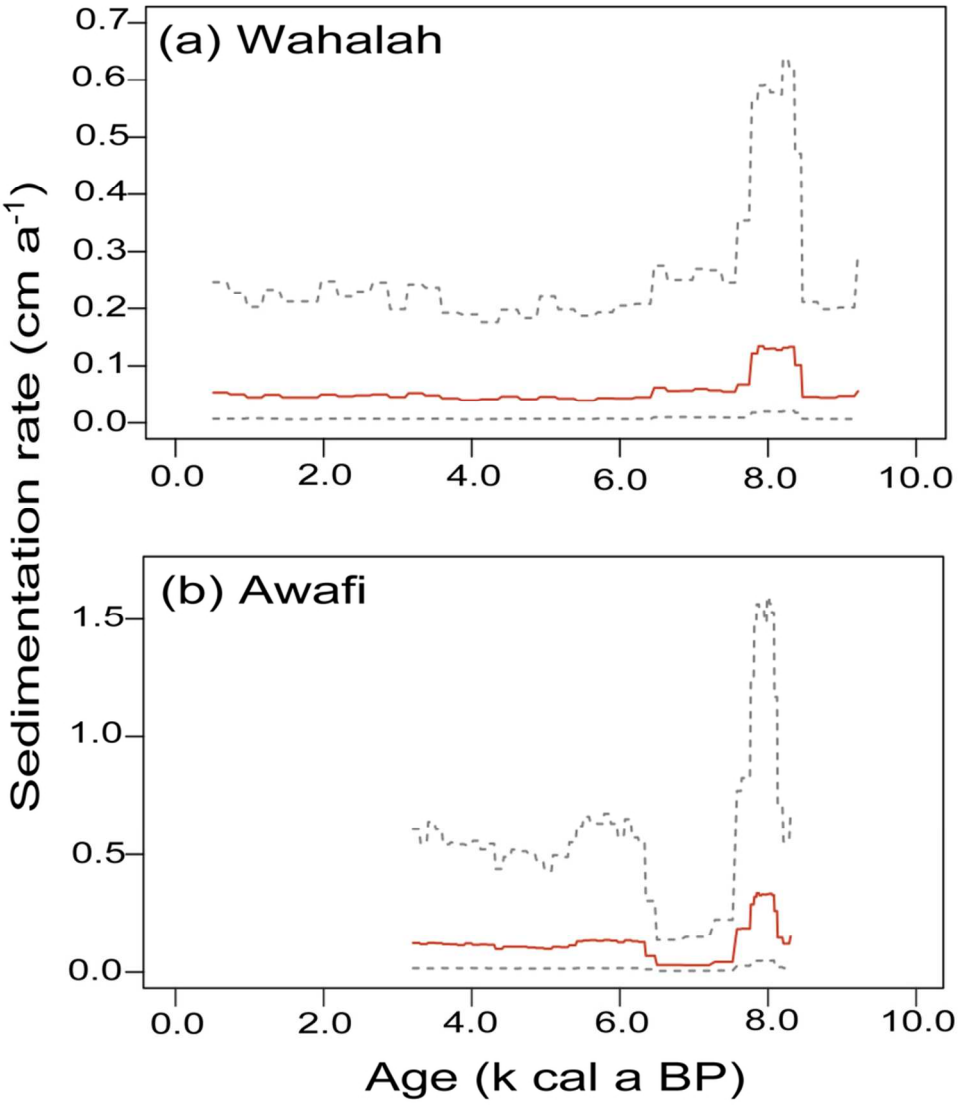

Figure 6: Sedimentation rates for (a) Wahalah and (b) Awafi with ages derived from the mean age-depth model for each site (refer to Fig. 5). Solid lines are the mean MCMC-derived sedimentation rates and dashed lines are the 95% confidence intervals.
85x99mm (300 x 300 DPI)

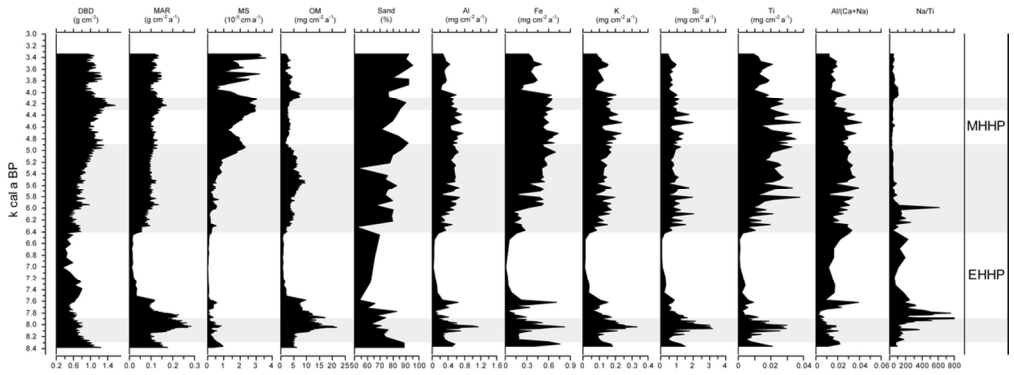

Figure 7: Sediment flux records for Awafi showing the key palaeoclimatic periods. The darker grey bands indicate periods of increased sediment flux and climatic aridity as discussed in the text.
105x38mm (300 x 300 DPI)

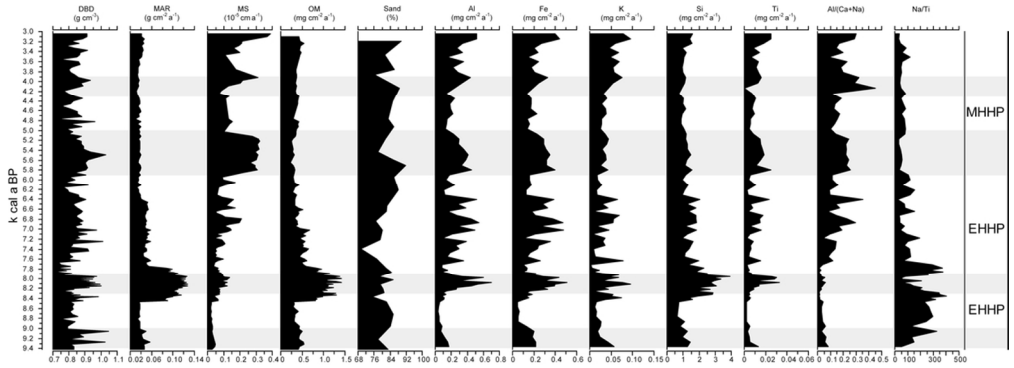

Figure 8: Sediment flux records for Wahalah showing the key palaeoclimatic periods. The darker grey bands indicate periods of increased sediment flux and climatic aridity as discussed in the text.
104x37mm (300 x 300 DPI)

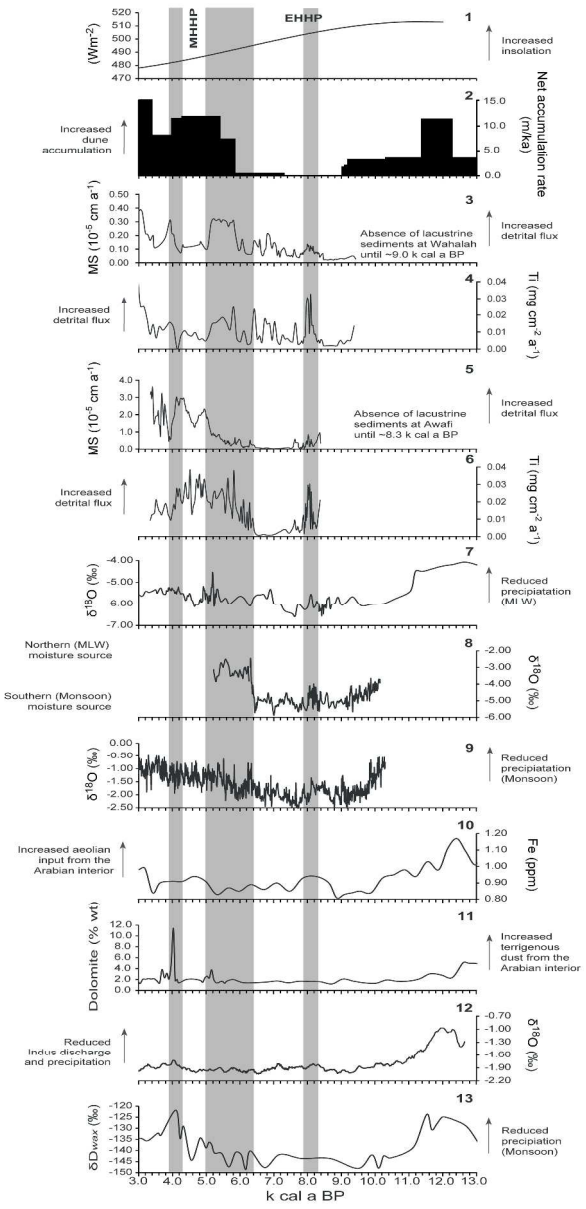

Figure 9: Comparison of palaeoclimate records from Arabia and surrounding regions (refer to Fig. 1 for the location of each site): (1) Insolation at 30°N (Berger and Loutre, 1991), (2) Dune net accumulation rates from SE Arabia (Leighton et al., 2014), (3) Wahalah MS signal (10-5 cm a-1), (4) Wahalah Ti flux record (mg cm-2a-1), (5) Awafi MS signal (10-5 cm a-1), (6) Awafi Ti flux record (mg cm-2a-1), (7) δ18O Soreq Cave speleothem record (Bar-Matthews et al., 2003), (8) δ18O Hoti Cave speleothem record (‰) (Neff et al., 2001), (9) δ18O Qunf Cave speleothem record (‰) (Fleitmann et al., 2007), (10) Iron (ppm) record from core 74KL, Arabian Sea (Sirocko et al., 1993), (11) Dolomite (%) record from core M5-422, Gulf of Oman (Cullen et al., 2000), (12) Globigerinoides ruber δ18O from core 63KA, Arabian Sea (Staubwasser et al., 2003), (13) δDwax record from core P178-15P, Gulf of Aden (Tierney and deMenocal, 2013). The key palaeoclimatic periods discussed in the text are shown.
292x533mm (300 x 300 DPI)